Construction and Building Materials 264 (2020) 120665

Contents lists available at ScienceDirect

Construction and Building Materials

journal homepage: www.elsevier.com/locate/conbuildmat

Effect of hydrophobicity on autogenous shrinkage and carbonation of alkali activated slag

Z.Y. Qu [a,b], F. Gauvin [b], F.Z. Wang [a,*], G. Liu [b,*], H.J.H. Brouwers [a,b]

[a] State Key Laboratory of Silicate Materials for Architectures, Wuhan University of Technology, Wuhan 430070, PR China
[b] Department of the Built Environment, Eindhoven University of Technology, P.O. Box 513, 5600 MB Eindhoven, PR China

HIGHLIGHTS

- The addition of s-slag can reduce the autogenous shrinkage of AAS.
- The s-slag shows a significant influence on the hygroscopic and water absorption properties.
- The resistance to carbonation of AAS can be improved after using s-slag.

ARTICLE INFO

Article history:
Received 8 May 2020
Received in revised form 3 August 2020
Accepted 18 August 2020
Available online 6 September 2020

Keywords:
Hydrophobic modification
Autogenous shrinkage
Alkali-activated slag
Carbonation resistance

ABSTRACT

The aim of this study is to investigate the feasibility of applying super-hydrophobic slag (s-slag) to reduce the autogenous shrinkage and enhance resistance to carbonation of alkali-activated slag (AAS). The s-slag is produced by milling slag with stearic acid. The influence of the s-slag on the wetting behaviour is characterized by the water contact angle. It was found that the addition of s-slag has a significant influence on the hygroscopic and water absorption properties of the AAS. The hydration kinetics, reaction products, internal humidity, surface tension of pore solution and carbonation depth are investigated in order to explain the mitigation mechanism of the autogenous shrinkage and carbonation test. After applying 20% s-slag, the autogenous shrinkage and carbonation depth of AAS can be reduced by 68% and 70%, respectively compared to the reference. The surface coating by stearic acid reduces the contact between the slag and the activated solution, which decreases the heat release of AAS. The hydrophobic modification alters the wetting property of the AAS which is helpful to decrease the capillary pressure and obstruct contact with CO_2. As a result, the autogenous shrinkage and carbonation depth are dramatically decreased. In addition, the introduction of the s-slag increases the compressive strength and flexural strength of AAS.

1. Introduction

Concrete is the most widely used artificial material in the world, and ordinary Portland cement (OPC) is the most general cementitious material in concrete manufacture [1;2,3,4,5,6,7,8]. However, the production of OPC involves high energy costs and a large amount of emissions of greenhouse gases [9,10,11]. In order to reduce the environmental impacts and natural resource consumption of cement production, alternative cementitious materials are considered [12–13,14]). Over the past decades, lots of research has been conducted on alkali-activated slag (AAS) due to the low energy consumption and a satisfied engineering performance compared to OPC [15,16,17,18].

Many studies have confirmed that AAS can develop comparable or even better mechanical properties of concrete than using normal cement [16,19,20,18]. However, until so far, the large scale application of the AAS is still limited due to the poor resistance performance to carbonation and the high autogenous shrinkage [15,19,18]. It has been reported that the carbonation resistance of AAS concrete was much lower compared to OPC when exposed to an environment composed of 10% to 20% of CO_2 at 70% relative humidity (RH) [21–22]. The low resistance to carbonation was generally identified to be induced by the lack of calcium hydroxide as pH buffer compared to OPC, on the other hand, the potential high shrinkage of AAS may cause cracks for CO_2 penetration. Malolepszy et al. found that the shrinkage of AAS mortars is 1.6 times higher as compared to OPC mortars [23], which increases the risk of reducing the resistance to carbonation. Therefore, it is necessary to find a

* Corresponding authors.
E-mail addresses: fzhwang@whut.edu.cn (F.Z. Wang), G.Liu@tue.nl (G. Liu).

https://doi.org/10.1016/j.conbuildmat.2020.120665
0950-0618/

method to mitigate the drawbacks of AAS and to achieve large scale applications.

In order to improve the durability performance of the AAS, numerous investigations have been conducted by applying various methods [21–22,19,24,25,18]. Some studies have focused on the carbonation of AAS whereas others focused on the shrinkage properties. Sumensh et al. investigated the effects of nano-materials on the carbonation of geopolymers [23]. It is concluded that the addition of the nano-particles such as nano-TiO_2 could refine the pore structure hindering the penetration of water and CO_2, then resulting in a decrease of carbonation depth [23]. The application of slag with higher MgO contents is also useful because of the formation of layered double hydroxides which have the capacity to bind CO_2 [22]. Palacios et al. investigated[24] the effects of the shrinkage-reducing admixtures on the properties of alkali-activated slag mortars and pastes. Polypropylene glycol-based shrinkage-reducing admixtures can reduce autogenous shrinkage by 85% and drying shrinkage by 50% in water glass-activated slag mortars [24]. Kumarappa et al. applied pre-wetted lightweight aggregates to mitigate the shrinkage of AAS [26]. The pre-wetted lightweight aggregates act as an internal curing agent which can control the development of autogenous shrinkage in AAS mortars [26]. However, the most common methods aim at the improvement of the carbonation and shrinkage behaviour by changing mixture design. Until so far, no positive result was reported based on the surface modification of raw materials for improving both shrinkage and carbonation performance.

Hydrophobic modification has been applied to improve the durability of cementitious materials [27,25,28]. Due to the porous microstructure of the hardened cement paste, most often occurring mechanisms of deterioration of concrete are related to the penetration of fluids [29,30,31]. The hydrophobic treatment can alter wetting behaviour within internal pores or cracks which increases the water absorption resistance of cementitious materials [28]. Among the integral water-resisting admixtures, stearic acid has attracted lots of attention due to its low price and good hydrophobic property [25,28]. Wong et al. found that the addition of stearic acid coated waste paper sludge ash could reduce water absorption of concrete by 84% [28]. Our previous study found that the addition of stearic acid coated slag could decrease the chloride penetration of lightweight concrete by 90% [25]. As water transport in the concrete plays a key role in the determination of the carbonation, hydrophobic modification has the potential to improve the carbonation resistance of AAS [23;21,20]. Furthermore, the wetting property of the pore walls has a big influence on internal humidity which is the driving force of the autogenous shrinkage of AAS [25,28]. Kumarappa et al [26]investigated the mechanism of autogenous shrinkage of alkali activated slag mortars. They concluded that the drastic drop in the internal relative humidity was the main reason for the important increase in the shrinkage values of AAS [26]. As reported by Shahidzadeh-Bonn et al. [32], a hydrophobic glass beads-based porous system presented a capillary stress of only one-tenth of the hydrophilic ones as the radius of menisci is dramatically increased because of the hydrophobicity. Therefore, hydrophobic modification has the potential to maintain the internal humidity of the cementitious materials and in turn, decrease the shrinkage of AAS. So far, the existing strategies for hydrophobic modification of concrete mainly involved additional surface treatment or bulk modification. As concrete surface suffers the threat of cracks, bulk modification is ideal for the hydrophobic enhancement of cementitious materials.

The aim of this study is to evaluate the feasibility of applying super-hydrophobic slag powder as a partial binder in order to mitigate the autogenous shrinkage and carbonation of AAS. The influence of the s-slag to wetting behaviour and water absorption are investigated which are related to the carbonation resistance of AAS. The hydrophobic performance of AAS is evaluated by the water contact angle value. In order to know the mitigation mechanism of the autogenous shrinkage, the internal humidity, surface tension of pore solution are also investigated.

2. Experiments

2.1. Materials

The ground granulated blast furnace slag (GGBS) is supplied by ENCI (the Netherlands). The elemental composition of the GGBS is determined by X-ray fluorescence, as: 34.61% SiO_2, 37.63% CaO, 13.26% Al_2O_3, 9.94% MgO, 0.47% Fe_2O_3, 1.24% SO_3, 0.47% K_2O, 0.98% TiO_2, 0.01% Cl, and 0.46% L.O.I. The superhydrophobic slag is prepared through a ball milling method for 1 h (100 rpm) using 1% stearic acid as a hydrophobic surface functionalizing agent as reported in our previous work [25]which is the optimum processing conditions to prepare the superhydrophobic slag (the slag without stearic acid is prepared with the same procedure). The resultant s-slag possesses a water contact angle (WCA) of 153° which can be classified as super-hydrophobic [33]. The activator is prepared by using the sodium hydroxide pellets, and commercial sodium silicate solution (27.69% SiO_2, 8.39% Na_2O and 63.92% H_2O by mass). The designed activators are prepared by mixing an appropriate amount of sodium hydroxide pellets into the sodium silicate solution and then cooling down to room temperature before casting. The equivalent Na_2O content is 6.2% by the mass of slag. The activator modulus and water/binder ratio are kept constant as 1.2 and 0.45, respectively. The dosage with the s-slag is 10%, 20% and 30% as shown in Table 1.

2.2. Testing methods

2.2.1. Calorimetric test

The influence of the s-slag on the hydration of the AAS is investigated by a TAM Air isothermal calorimeter. The reaction kinetic experiments are carried out for 80 h and the temperature of the measuring cells is kept at 20 ℃. The calorimetry results are normalized per gram of solid powders (slag and s-slag).

2.2.2. Mechanical properties

The flexural and compressive strength of the AAS samples with a curing age of 7, 14 and 28 days are determined according to EN 196–1 standard [34]. The samples are cured in a climate room (20 ℃ and RH 50%) sealed with plastic wrap. $40 \times 40 \times 160$ mm^3 samples are used for the flexural strength test and $40 \times 40 \times 40$ mm^3 samples are used for the compressive strength test.

2.2.3. Water absorption

The capillary water absorption of the AAS and hydrophobic modification AAS is tested according to EN 480–5 [35]. AAS samples with 28 days curing age are used for the capillary water absorption test. All of the samples are immersed under the water with a depth of about 3 mm for 43 days. A digital balance is used to measure the mass of the AAS samples periodically during the water absorption test.

2.2.4. Sessile drop test

Sessile drop method is applied the measure the water contact angle with a piece of AAS samples curing 1 day with a diameter of 5 cm.

Table 1
Mixture proportions of AAS pastes with different dosages of S-slag.

Mixture	Slag (g)	S- slag (g)	SiO_2 (mol)	Na_2O (mol)	H_2O (g)
Ref	1000	0	1.2	1	450
H-10%	900	100	1.2	1	450
H-20%	800	200	1.2	1	450
H-30%	700	300	1.2	1	450

2.2.5. Extraction of the pore solution and surface tension tests

Pore solution of hardened AAS paste is obtained by squeezing the cubic specimens with a pressure of 70 MPa. The surface tension of the pore solution at 1 d and 7d measured with a surface tension analyser. The surface tension of distilled water by the analyser is 72.22 dyne/cm.

2.2.6. Internal humidity

The internal relative humidity (RH) of AAS mortars is measured by Hygropin moisture meter (Newa Techniek B.V.) with in-situ RH sensor probes. The measuring sleeves with 6 cm depth are embedded in the fresh mortar in a 10 × 10 × 10 cm^3 mould and the surface of the cast samples are sealed with plastic wrap. The internal RH is tested every day over a period of 28 days. Three replicate measurements are recorded to calculate the average internal RH.

2.2.7. Autogenous shrinkage measurements

The autogenous deformation test is measured according to ASTM C 1698–09 [36]by corrugated polyethylene tubes with a length of 420 mm and a diameter of 29 mm. All of the AAS samples are stored in a stable environment with 20 °C.

2.2.8. Carbonation test

The AAS is cast into a cylinder mould with a diameter of 10 cm and a depth of 6 cm. After casting, the AAS samples are covered with plastic wrap and stored in the climate room (20 ℃ and RH 50%) until testing. After curing for 28 days, the bottom and sides of the cylinder surface are coated with epoxy to allow CO_2 ingress only from the lateral cast surfaces. The AAS samples are moved to the carbonation test chamber with a setting of 20 °C, 65% RH with a 20% CO_2 concentration. The test duration is 2 weeks. The carbonation depth of sample is identified by using spraying of phenolphthalein (1% with absolute ethyl alcohol).

3. Results and discussion

3.1. Reaction kinetics

The heat evolution and total heat release of the AAS samples are shown in Fig. 1 (a) and (b). The heat release curves present four reaction stages similar to Portland cement-based materials and other previous research on AAS (Z. [3,37]. The characteristic peak of the acceleration period is located at about 5 h which is in line with the AAS reported in other research. It can be seen that with the addition of the s-slag, the acceleration peak of AAS exhibits lower intensity which is in accordance with the influence of the s-slag to the OPC [25]. This can be attributed to the surface coating of stearic acid which decreases the contact between the alkaline solution and slag. The stearic acid coating decreases the reaction between slag and the alkaline solution which in turn decreasing the heat release. This is in line with the cumulative heat evolution of the AAS samples. The s-slag contained samples that present a lower total heat release. However, the addition of s-slag did not change the reaction process as it can be seen that the duration of each period of the AAS samples is the same[25].

3.2. Reaction products

The FTIR spectra of the AAS are shown in Fig. 2 (a). All the AAS samples present similar patterns which indicates that the reaction products formed are similar. The peaks at 3305 cm^{-1} and 1640 cm^{-1} belong to water [38]. It should be noted that the AAS containing s-slag present two bands at 2916 cm^{-1} and 2848 cm^{-1}. These are attributed to the asymmetric stretching vibration and symmetrical stretching vibration of C–H bonds as the stearic acid contains many $–CH_2$ groups in its structure [25,38]. The intensity of these two peaks is very weak as the stearic acid content is quite low in the AAS. The bands at 940 cm^{-1} can be assigned to the formation of calcium aluminosilicate hydrate which is one type of C-A-S-H gel (Z. [3]. The bands at 872 cm^{-1} and 641 cm^{-1} are attributed to the deformational vibrations of Si-O-Si or Si-O-Al [38]. The XRD results of the AAS samples are shown in Fig. 2 (b). All the samples present similar XRD patterns that confirm the FTIR results. The main phases are hydrotalcite as well as C-A-S-H with a minor amount of portlandite [39]. Based on the FTIR and XRD results, it can be concluded that the addition of the s-slag does not change the reaction products of the AAS.

3.3. Mechanical property

The compressive and flexural strength of the AAS pastes is shown in Fig. 3 (a) and (b). It should be noted that the influences of s-slag on the compressive strength and flexural strength are different. As shown in Fig. 3 (a), the incorporation of the s-slag results in a continuous decrease of the compressive strength from 61.81 MPa to 52.61 MPa at 1 d, from 81.14 MPa to 71.64 MPa at 7 d and from 94.4 MPa to 83.72 MPa at 28 d. This is due to the less formation of the reaction products as the coating of stearic acid reduces the contact between the slag and activator which is in line with the results of influence to the heat release as shown in Fig. 1 (a). On the contrary, the incorporation of s-slag increases the flexural strength of the AAS from 3.56 MPa to 4.72 MPa at 7d and from 3.81 MPa to 6.03 MPa at 28 d as shown in Fig. 3 (b). This can be attributed to the mitigation of micro-cracks development through the addition of the s-slag. As reported by previous studies [40]; Z. [3,41], AAS suffering a high risk of micro-cracks due to the high rate of autogenous shrinkage while flexural strength is more sensitive to the micro-cracks than the compressive strength. This indicates that the addition of s-slag may also contribute to the reduction of the micro-cracks development in alkali activated slag systems.

3.4. Internal humidity and surface tension of the pore solution

The influences of s-slag dosages on the internal RH of AAS are presented in Fig. 4 (a). The internal RH decreases with the time increasing for all samples which can be attributed to the continuous hydration of the slag [28, 32]. However, the addition of s-slag significantly retards the reduction of the internal humidity of the AAS. At 1d, the reference sample presents an internal humidity value of around 85% which is lower than the other samples. Then it has a quick decrease to around 72% at 7d and then it continuously decreases to around 67% at 28d. With s-slag incorporation,

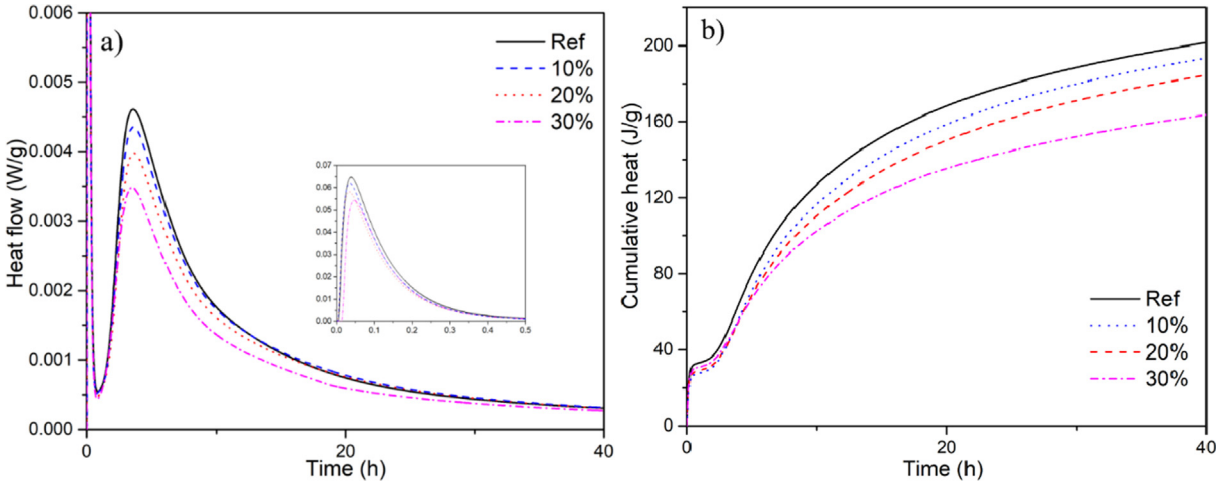

Fig. 1. Normalized heat flow (a) and cumulative heat release (b) of the AAS paste with different dosages of s-slag.

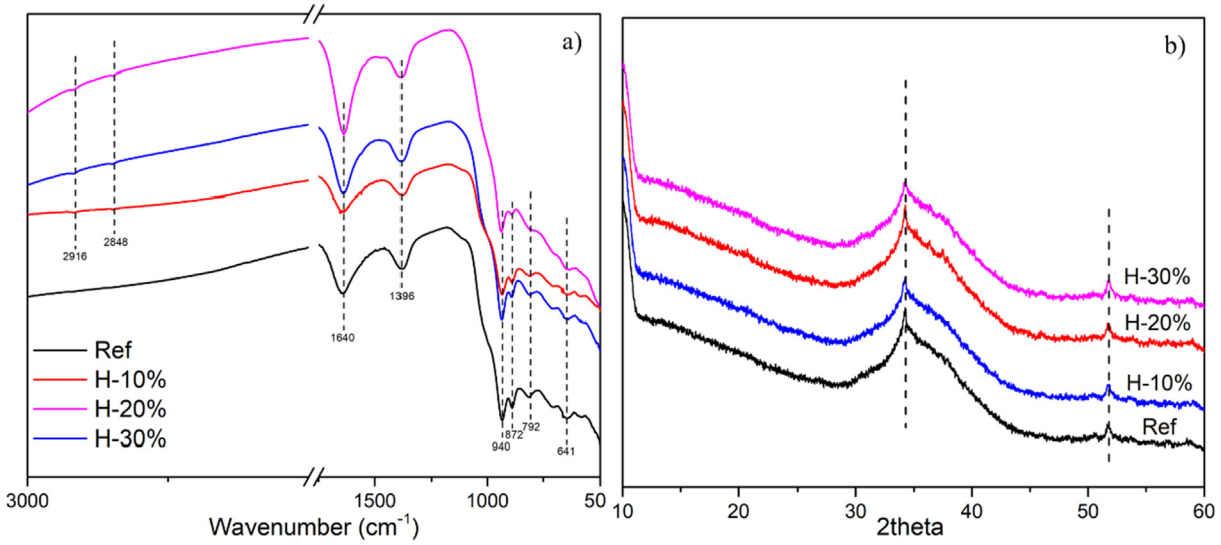

Fig. 2. FTIR (a) and XRD (b) spectra of the alkali-activated slag.

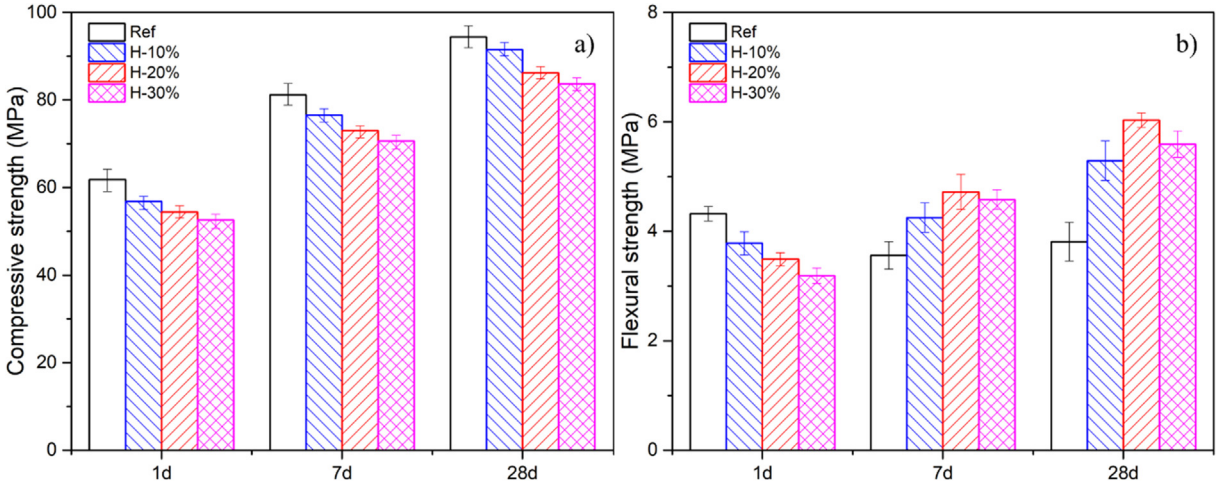

Fig. 3. Compressive strength (a) and flexural strength (b) of AAS pastes.

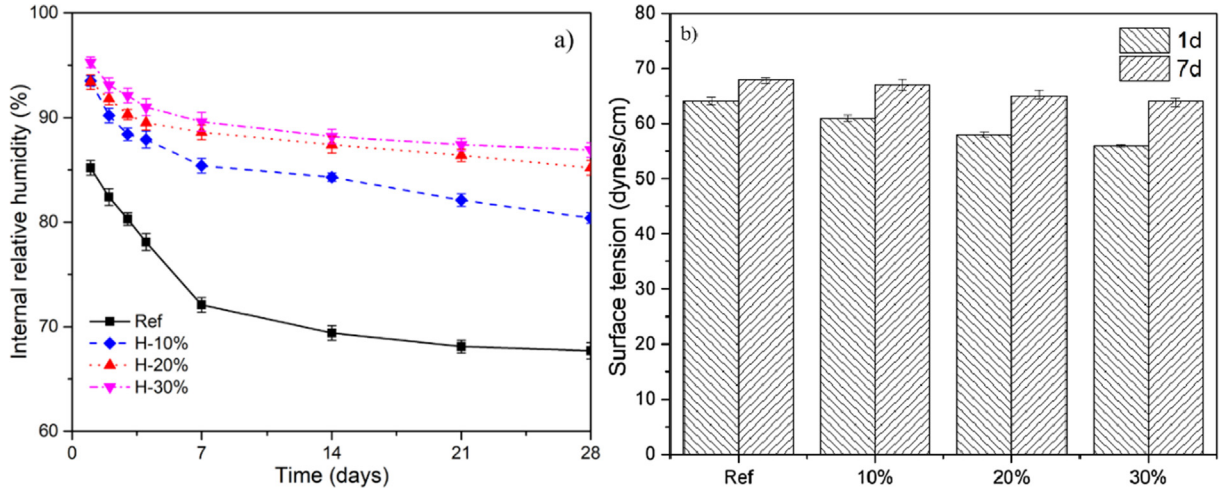

Fig. 4. Internal humidity (a) and surface tension (b) of the pore solution of AAS.

the humidity decreases much more slowly. For the H-30% sample, the internal humidity is 96% at 1d and then slightly decreases to 90% at 28d. According to the Kelvin and Laplace equations, higher internal humidity results in a lower pore pressure which is beneficial for the mitigation of the autogenous shrinkage of AAS [26]; Z. [3]. Usually, the surface tension of pore solution plays a key role in the determination of the internal humidity and reduction of the surface tension of pore solution is a usual strategy to maintain the internal humidity to mitigate the autogenous shrinkage of AAS [42]; Z. [3,43]. In order to figure out the mechanism of the slow humidity drop, the surface tension of the pore solution of the AAS is analyzed as shown in Fig. 4 (b). It can be seen that for all the AAS samples, the surface tension increases from 1d to 7d which is also observed in a previous study [26]. This can be attributed to the continuous hydration of the AAS and more ions were released from the slag to the pore solution [26]; Z. [3]. The addition of s-slag seems to slightly reduce the surface tension due to the lower reaction intensity compared to reference as shown in Fig. 1. The differences of the surface tension from the different samples are not obvious which is not the cause of the retardation of the internal humidity drop.

3.5. Wetting property and autogenous shrinkage behavior

The results of water contact angles and autogenous shrinkage of the AAS as a function of time are shown in Fig. 5. As hydrophilic material, the original water contact angle of AAS is 0 which is not listed in Fig. 5 (a). The water contact angle of AAS with 10% replacement is 32° and then the water contact angle presents a sharp increase to 79° and 81° at 20% and 30% replacements, respectively. It should be noted that the decrease of the autogenous shrinkage presents a similar pattern as shown in Fig. 5 (b). The addition of super-hydrophobic slag results in the decrease of shrinkage of AAS in all mixtures. With a 10% replacement, the shrinkage deformation is reduced by 38% and it increases to 68% by 20% replacement. With 30% replacement, the autogenous shrinkage deformation decreases 70% which is close to the result of a 20% replacement. The results above indicate that the hydrophobic property has an influence on the shrinkage of the AAS. It can be seen with higher replacement (30%), the shrinkage decreases not that much which is in line with the hydrophobic property of the AAS. This indicates that AAS with a 20% replacement of s-slag is also an optimum amount to decrease the

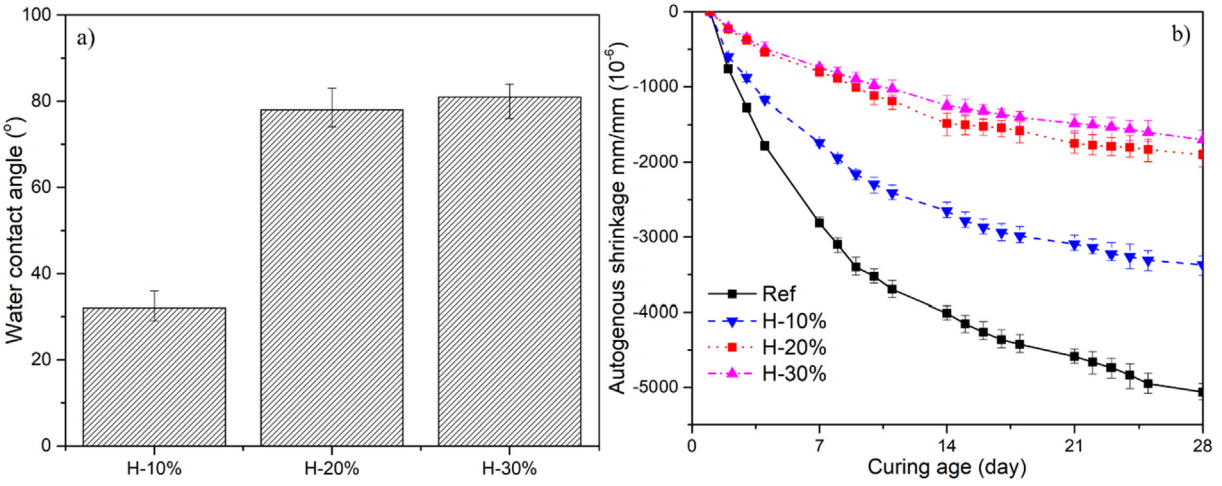

Fig. 5. Water contact angles and autogenous deformations of the AAS as a function of time.

autogenous shrinkage of AAS. As shown in Section 3.3.1, the addition of the s-slag did not change the surface tension of the pore solution that much which indicates that it is not the cause for the decrease of the autogenous shrinkage of AAS. On the other hand, the addition of s-slag changed the contact angle, consequently, the capillary stress can be influenced as well, which can result in the variation of shrinkage behavior. This will be further discussed in Section 3.7.

3.6. Carbonation resistance

The water absorption curves of the AAS pastes are shown in Fig. 6 (a). The addition of slag dramatically decreases the water absorption of the AAS. With a 10% replacement, the water absorption decreases by 32%. A sharp water absorption decrease can be seen at a higher replacement dosage. It decreases by 62% and 69% separately at 20% and 30% replacement. A plausible mechanism is that the s-slag reacts with the activators left the stearic acid on the surface of the internal pores or the s-slag bonds directly on the with the hydration products of the AAS and then the wetting property of the pore in the AAS are altered [28]. This decreases capillary suction and influences the liquid transport inside the AAS. It should be noted that with higher replacement (at 30%), the water absorption did not change much compared with 20% replacement. This is in line with the hydrophobic property changes of the AAS which illustrates that 20% addition of the superhydrophobic slag is enough to modify the AAS for hydrophobic function. Carbonation is a serious threat to the durability of AAS. The diffusion of CO_2 can change its initially strongly alkaline environment to lower pH values [44,45,46]. It has been concluded that AAS is prone to be damaged by carbonation compared with OPC under the same exposure conditions [47,48]. The results of carbonation depth are shown in Fig. 6 (b). It can be concluded that the addition of s-slag is beneficial to increase the carbonation resistance of the AAS. The reference sample presents a carbonation depth of 24 mm. All the hydrophobic modification samples present a lower carbonation depth especially with a 20% replacement of s-slag, the carbonation depth decreases 70%.

3.7. The modification mechanism by using super-hydrophobic coating slag in AAS

Generally, autogenous shrinkage occurs because of the internal moisture loss as the hydration proceeds and the water in the pore system of AAS is consumed from large pores to small pores. Then resulting in the formation of menisci between liquid and gas in the capillary pores and then capillary stress rises [49,43] as shown in Fig. 7 (a). The internal capillary stress can be calculated by the Young-Laplace equation:

$$\sigma = -\frac{2\gamma\cos\theta}{r} \tag{1}$$

and Kelvin equation:

$$In(RH_K) = -\frac{2\gamma M\cos\theta}{\rho rRT} \tag{2}$$

Where, σ is the capillary pressure in MPa, γ is the surface tension in N/m, θ is the water contact angle of the wall of the capillary pore, r is the radius of the pore in m, M is the molar volume of water which is 18 cm^3/mol, ρ is the pore solution density in kg/m^3 which is experimentally tested in this study, R is the universal gas constant which is 8.314 J/mol·K and T is the absolute temperature which is 293.15 K.

Normally, as hydrophilic materials, θ is taken the value of 0 and the pore radius is equal to the Kelvin radius which is shown in Fig. 7 (a). As the shape of the meniscus in the pore is concave, negative capillary pressure generates which is the driving force for the shrinkage of cementitious materials [49,43]. Traditional methods to decrease the autogenous shrinkage includes internal curing, which can supply more water or addition of the shrinkage reducing admixtures (SRA), which can decrease the surface tension of the pore solution. However, the influence of the wetting property in cementitious materials has not been investigated systematically, as such, a parametric investigation is performed in this study to see how contact angle influences the internal relative humidity and capillary pressure. The influence of s-slag contents on relative humidity and capillary pressure as a function of pore radius is shown in Fig. 8 (a) and (b). It can be seen that the influence of s-slag contents on internal humidity and capillary pressure is mainly performed on the pores with a radius of less than 50 nm which belongs to the capillary pores. This is in line with the previous study [50,51,43], finer pores generate higher capillary stress resulting in higher autogenous or drying shrinkage. In this range of pores, with enhanced hydrophobic property, meniscus curvature increases as shown in Fig. 7 (b). Then the internal RH rises, and the capillary pressure drops with the increase of the water contact angle which is consistent with the evolution of internal relative humidity results in Fig. 3 (a). The decrease of the capillary pressure results in the mitigation of the autogenous shrinkage of the AAS.

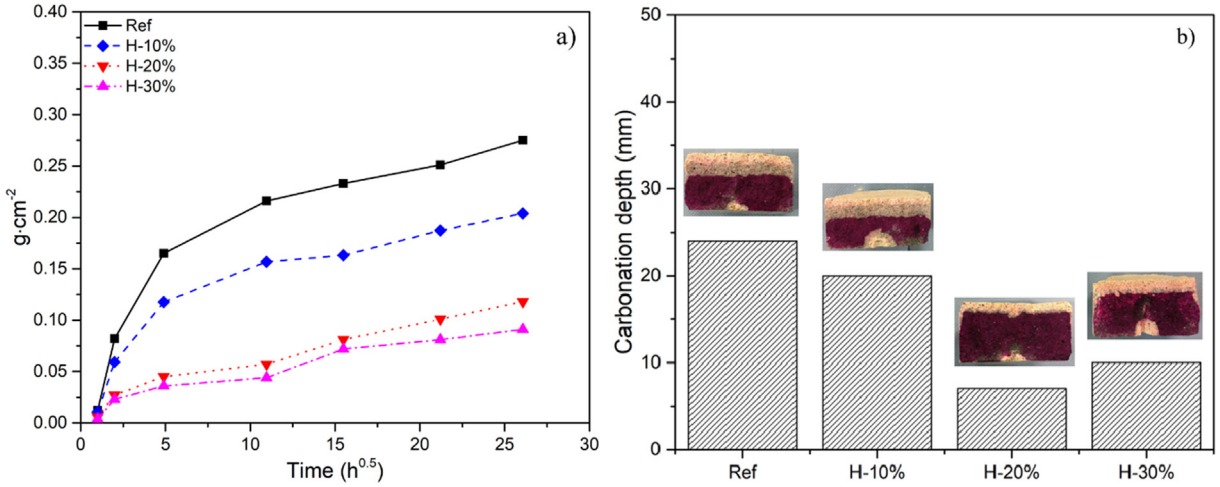

Fig. 6. Water absorption (a) and carbonation depth (b) of the AAS samples.

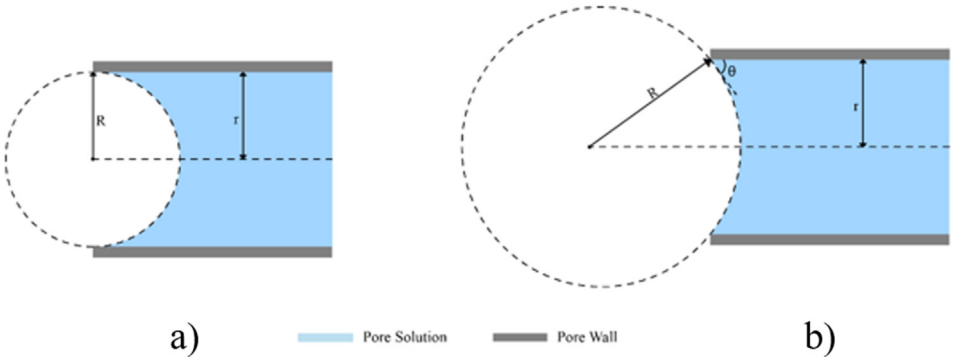

Fig. 7. The shape of the menisci in the pores and capillary stress with different water contact angles (θ): a) θ = 0°, b) 0° < θ < 90°.

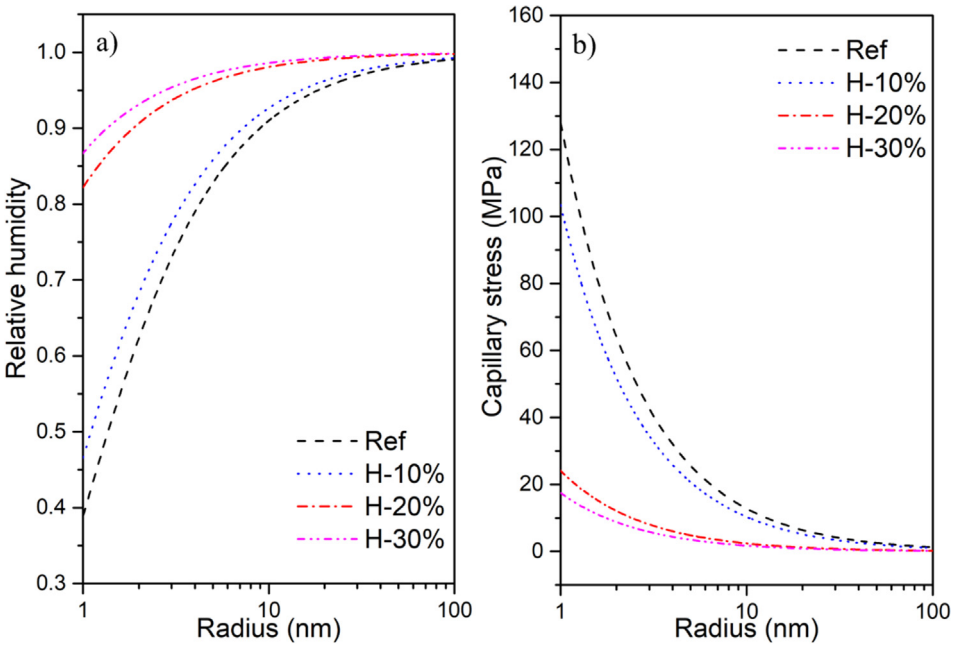

Fig. 8. Evolution of relative humidity (a) and capillary pressure (b) as a function of the pore radius for different contact angles.

On the other hand, the humidity and pore structure are the key factors of resistance to carbonation for alkali activated materials [52]. The moisture is necessary for the occurrence of the carbonation reaction because CO_2 needs to be dissolved in water, at first carbonic acid is formed, then react with Ca^{2+} leached from calcium hydrate or C-A-S-H gel [44,45]. Usually, when the relative humidity is high enough, for example at RH > 80%, the pores or tunnel for gas penetration can be clogged by the excess water [53]. Combining the presented results, the addition of s-slag significantly increases the internal humidity of AAS samples, which subsequently slows down the CO_2 transportation, then presented as a decreased carbonation depth. Furthermore, the increased water contact angle reduces the contact between water and reaction products, which further inhibit the reaction of carbonation. Especially, the reduction of the autogenous shrinkage lowers the micro-cracks' formation (identified as enhanced flexural strength), which reduces the risk of the fast CO_2 penetration. These all promote the resistance to carbonation of AAS containing s-slag.

4. Conclusions

This study investigated the influence of superhydrophobic slag (s-slag) on a wide range of properties of AAS. In addition, the mitigation mechanism of the autogenous shrinkage of AAS by s-slag were studied, based on a new mitigation strategy of the shrinkage of AAS.

1. The addition of s-slag is efficient to decrease the autogenous shrinkage of the AAS. At 28 days, the autogenous shrinkage of AAS is decreased by 68% and 70% with 20% and 30% replacement. This is in line with the results of the water contact angle and water absorption test. It illustrates that the 20% replacement is sufficient to make the AAS hydrophobic.
2. The mitigation of the autogenous shrinkage is attributed to the increase of the hydrophobicity which limits the drop of internal humidity of AAS resulting in a decrease of capillary stress.
3. The carbonation depth of the AAS is decreased after the addition of s-slag. At 20% replacement, the carbonation depth is decreased by 70% which is in line with the results of water absorption.
4. The heat release and compressive strength of the AAS is decreased due to less formation of reaction products. The flexural strength of the AAS is increased as the micro-cracks of the AAS is reduced.

This work presents a new way to mitigate the shrinkage of AAS at the same time decreasing the carbonation. Through the addition

of superhydrophobic slag, the hydrophobicity of the AAS is increased which results in the increase of the shrinkage and carbonation resistance. Given the low cost and facile preparation of the s-slag, this bulk hydrophobic modification methods have excellent potential for the large scale application of AAS.

CRediT authorship contribution statement

Z.Y. Qu: Conceptualization, Methodology, Validation, Writing - original draft. **F. Gauvin:** Writing - review & editing. **F.Z. Wang:** Writing - review & editing. **G. Liu:** Writing - review & editing. **H. J.H. Brouwers:** Writing - review & editing, Supervision.

Declaration of Competing Interest

The authors declare that they have no known competing financial interests or personal relationships that could have appeared to influence the work reported in this paper.

Acknowledgements

The authors would like to acknowledge the financial support by STW-foundation and TU Eindhoven for funding this research. Mrs. A.C.A. Delsing in the lab of Building Physics and Services at the Eindhoven University of Technology is acknowledged for providing experimental support on the SEM analysis. Furthermore, the authors wish to express their gratitude to the following sponsors of the Building Materials research group at TU Eindhoven: Rijkswaterstaat Grote Projecten en Onderhoud; Graniet-Import Benelux; Kijlstra Betonmortel; Struyk Verwo; Attero; Enci; Rijkswaterstaat Zee en Delta-District Noord; Van Gansewinkel Minerals; BTE; V. d. Bosch Beton; Selor; GMB; Icopal; BN International; Eltomation; Knuaf Gips; Hess AAC Systems; Kronos; Joma; CRH Europe Sustainable Concrete Centre; Cement & Beton Centrum; Heros; Inashco; Keim; Sirius International; Boskalis; NNERGY; Millvision; Sappi and Studio Roex (in chronological order of joining).

References

[1] X. He, Z. Zheng, J. Yang, Y. Su, T. Wang, B. Strnadel, Feasibility of incorporating autoclaved aerated concrete waste for cement replacement in sustainable building materials, J. Clean. Prod. 250 (2020).
[2] N. Li, C. Shi, Z. Zhang, Understanding the roles of activators towards setting and hardening control of alkali-activated slag cement, Compos. Part B Eng. 171 (2019) 34–45.
[3] Z. Li, M. Nedeljković, B. Chen, G. Ye, Mitigating the autogenous shrinkage of alkali-activated slag by metakaolin, Cem. Concr. Res. 122 (2019) 30–41.
[4] Y. Ma, X. Yang, J. Hu, Z. Zhang, H. Wang, Accurate determination of the "time-zero" of autogenous shrinkage in alkali-activated fly ash/slag system, Compos. Part B Eng. 177 (2019).
[5] B. Panda, S. Ruan, C. Unluer, M.J. Tan, Investigation of the properties of alkali-activated slag mixes involving the use of nanoclay and nucleation seeds for 3D printing, Compos. Part B Eng. 186 (2020).
[6] Z. Sun, X. Lin, P. Liu, D. Wang, A. Vollpracht, M. Oeser, Study of alkali activated slag as alternative pavement binder, Constr. Build. Mater. 186 (2018) 626–634.
[7] L. Wang, L. Chen, D.C.W. Tsang, Y. Zhou, J. Rinklebe, H. Song, E.E. Kwon, K. Baek, Y.S. Ok, Mechanistic insights into red mud, blast furnace slag, or metakaolin-assisted stabilization/solidification of arsenic-contaminated sediment, Environ. Int. 133 (2019).
[8] J. Yang, J. Huang, Y. Su, X. He, H. Tan, W. Yang, B. Strnadel, Eco-friendly treatment of low-calcium coal fly ash for high pozzolanic reactivity: A step towards waste utilization in sustainable building material, J. Clean. Prod. 238 (2019).
[9] J.L. Provis, J.S.J. Van Deventer, Alkali activated materials: state-of-the-art report, RILEM TC 224-AAM, Springer Science & Business Media, 2013.
[10] C. Shi, B. Qu, J.L. Provis, Recent progress in low-carbon binders, Cem. Concr. Res. 122 (2019) 227–250.
[11] Z. Zhang, J.L. Provis, A. Reid, H. Wang, Geopolymer foam concrete: An emerging material for sustainable construction, Constr. Build. Mater. 56 (2014) 113–127.
[12] S.A. Bernal, R.M. de Gutiérrez, A.L. Pedraza, J.L. Provis, E.D. Rodriguez, S. Delvasto, Effect of binder content on the performance of alkali-activated slag concretes, Cem. Concr. Res. 41 (2011) 1–8.
[13] S.A. Bernal, J.L. Provis, B. Walkley, R. San Nicolas, J.D. Gehman, D.G. Brice, A.R. Kilcullen, P. Duxson, J.S.J. van Deventer, Gel nanostructure in alkali-activated binders based on slag and fly ash, and effects of accelerated carbonation, Cem. Concr. Res. 53 (2013) 127–144.
[14] J.L. Provis, S.A. Bernal, Geopolymers and related alkali-activated materials, Annu. Rev. Mater. Res. 44 (2014) 299–327.
[15] C.D. Atiş, C. Bilim, Ö. Çelik, O. Karahan, Influence of activator on the strength and drying shrinkage of alkali-activated slag mortar, Constr. Build. Mater. 23 (2009) 548–555.
[16] A. Fernández-Jiménez, J.G. Palomo, F. Puertas, Alkali-activated slag mortars: mechanical strength behaviour, Cem. Concr. Res. 29 (1999) 1313–1321.
[17] S.-D. Wang, K.L. Scrivener, Hydration products of alkali activated slag cement, Cem. Concr. Res. 25 (1995) 561–571.
[18] V. Živica, Effects of type and dosage of alkaline activator and temperature on the properties of alkali-activated slag mixtures, Constr. Build. Mater. 21 (2007) 1463–1469.
[19] M. Palacios, F. Puertas, Effect of shrinkage-reducing admixtures on the properties of alkali-activated slag mortars and pastes, Cem. Concr. Res. 37 (2007) 691–702.
[20] F. Puertas, A. Fernández-Jiménez, M.T. Blanco-Varela, Pore solution in alkali-activated slag cement pastes. Relation to the composition and structure of calcium silicate hydrate, Cem. Concr. Res. 34 (2004) 139–148.
[21] S.A. Bernal, R.M. de Gutierrez, J.L. Provis, V. Rose, Effect of silicate modulus and metakaolin incorporation on the carbonation of alkali silicate-activated slags, Cem. Concr. Res. 40 (2010) 898–907.
[22] S.A. Bernal, J.L. Provis, D.G. Brice, A. Kilcullen, P. Duxson, J.S.J. van Deventer, Accelerated carbonation testing of alkali-activated binders significantly underestimates service life: The role of pore solution chemistry, Cem. Concr. Res. 42 (2012) 1317–1326.
[23] Andersson, R., Gram, H.-E., Malolepszy, J., Deja, J., 1988. Alkali-activated slag.
[24] M. Palacios, F. Puertas, Effect of superplasticizer and shrinkage-reducing admixtures on alkali-activated slag pastes and mortars, Cem. Concr. Res. 35 (2005) 1358–1367.
[25] Z.Y. Qu, Q.L. Yu, Synthesizing super-hydrophobic ground granulated blast furnace slag to enhance the transport property of lightweight aggregate concrete, Constr. Build. Mater. 191 (2018) 176–186.
[26] D.B. Kumarappa, S. Peethamparan, M. Ngami, Autogenous shrinkage of alkali activated slag mortars: Basic mechanisms and mitigation methods, Cem. Concr. Res. 109 (2018) 1–9.
[27] J. De Vries, R.B. Polder, Hydrophobic treatment of concrete, Constr. Build. Mater. 11 (1997) 259–265.
[28] H.S. Wong, R. Barakat, A. Alhilali, M. Saleh, C.R. Cheeseman, Hydrophobic concrete using waste paper sludge ash, Cem. Concr. Res. 70 (2015) 9–20.
[29] H. Du, S. Du, X. Liu, Effect of nano-silica on the mechanical and transport properties of lightweight concrete, Constr. Build. Mater. 82 (2015) 114–122.
[30] Z.Y. Qu, Q.L. Yu, H.J.H. Brouwers, Relationship between the particle size and dosage of LDHs and concrete resistance against chloride ingress, Cem. Concr. Res. (2018).
[31] Y. Zhang, M. Zhang, G. Ye, Influence of moisture condition on chloride diffusion in partially saturated ordinary Portland cement mortar, Mater. Struct. 51 (2018) 36.
[32] N. Shahidzadeh-Bonn, A. Azouni, P. Coussot, Effect of wetting properties on the kinetics of drying of porous media, J. Phys. Condens. matter 19 (2007).
[33] C. Spathi, N. Young, J.Y.Y. Heng, L.J.M. Vandeperre, C.R. Cheeseman, A simple method for preparing super-hydrophobic powder from paper sludge ash, Mater. Lett. 142 (2015) 80–83.
[34] BS-EN-196-1. Methods of testing cement – Part 1: determination of strength, 2005. . Br. Stand. Institution-BSI CEN Eur. Comm. Stand. https://doi.org/10.1111/j.1748-720X.1990.tb01123.x
[35] EN, B.S., 1997. 480-5. Tests methods, determination of capillary absorption. Br. Stand. Inst.
[36] ASTM, C., 2009. 1698-09,'. Stand. Test Method Autogenous Strain Cem. Paste Mortar', Am. Soc. Test. Mater. ASTM Int.
[37] Z. Shi, C. Shi, S. Wan, Z. Zhang, Effects of alkali dosage and silicate modulus on alkali-silica reaction in alkali-activated slag mortars, Cem. Concr. Res. 111 (2018) 104–115.
[38] B. Yuan, Q.L. Yu, H.J.H. Brouwers, Reaction kinetics, reaction products and compressive strength of ternary activators activated slag designed by Taguchi method, Mater. Des. 86 (2015) 878–886.
[39] Z. Sun, A. Vollpracht, Isothermal calorimetry and in-situ XRD study of the NaOH activated fly ash, metakaolin and slag, Cem. Concr. Res. 103 (2018) 110–122.
[40] F. Collins, J.G. Sanjayan, Cracking tendency of alkali-activated slag concrete subjected to restrained shrinkage, Cem. Concr. Res. 30 (2000) 791–798.
[41] J.J. Thomas, A.J. Allen, H.M. Jennings, Density and water content of nanoscale solid C-S–H formed in alkali-activated slag (AAS) paste and implications for chemical shrinkage, Cem. Concr. Res. 42 (2012) 377–383.
[42] Kotrla, J., Soukal, F., Bilek, V., Alexa, M., 2019. Effects of shrinkage-reducing admixtures on autogenous shrinkage in alkali-activated materials, in: IOP Conference Series: Materials Science and Engineering. IOP Publishing, p. 12023.
[43] H. Ye, A. Radlińska, Shrinkage mitigation strategies in alkali-activated slag, Cem. Concr. Res. 101 (2017) 131–143.
[44] T. Bakharev, J.G. Sanjayan, Y.-B. Cheng, Resistance of alkali-activated slag concrete to carbonation, Cem. Concr. Res. 31 (2001) 1277–1283.
[45] D.W. Law, A.A. Adam, T.K. Molyneaux, I. Patnaikuni, Durability assessment of alkali activated slag (AAS) concrete, Mater. Struct. 45 (2012) 1425–1437.

[46] K. Pasupathy, M. Berndt, A. Castel, J. Sanjayan, R. Pathmanathan, Carbonation of a blended slag-fly ash geopolymer concrete in field conditions after 8 years, Constr. Build. Mater. 125 (2016) 661–669.
[47] K. Behfarnia, M. Rostami, An assessment on parameters affecting the carbonation of alkali-activated slag concrete, J. Clean. Prod. 157 (2017) 1–9.
[48] N. Li, N. Farzadnia, C. Shi, Microstructural changes in alkali-activated slag mortars induced by accelerated carbonation, Cem. Concr. Res. 100 (2017) 214–226.
[49] J.K. Mackenzie, The elastic constants of a solid containing spherical holes, Proc. Phys. Soc. Sect. B 63 (1950) 2.
[50] P. Lura, O.M. Jensen, J. Weiss, Cracking in cement paste induced by autogenous shrinkage, Mater. Struct. 42 (2009) 1089–1099.
[51] H. Ye, C. Cartwright, F. Rajabipour, A. Radlińska, Understanding the drying shrinkage performance of alkali-activated slag mortars, Cem. Concr. Compos. 76 (2017) 13–24.
[52] Courard, L., Lucquiaud, V., 2017. Influence of hydrophobic treatments applications on the concrete carbonation delay, in: Proceedings of 14th International Conference on Durability of Building Materials and Components. pp. 403–404.
[53] L. De Ceukelaire, D. Van Nieuwenburg, Accelerated carbonation of a blast-furnace cement concrete, Cem. Concr. Res. 23 (1993) 442–452.